Thermochimica Acta, 210 (1992) 49–65
Elsevier Science Publishers B.V., Amsterdam

Thermodynamic study of molecular beam epitaxial growth of InGaAs/GaAs strained layer superlattices

M.R. Bruni, A. Lapiccirella, G. Scavia, M.G. Simeone and S. Viticoli
ITSE-CNR, c.p. 10000, 16 Monterotondo Stazione, Rome (Italy)

N. Tomassini
IMAI-CNR, c.p. 10000, 16 Monterotondo Stazione, Rome (Italy)

(Received 5 December 1991)

Abstract

A thermodynamic study on the molecular beam epitaxial (MBE) growth of binary GaAs, InAs and $Ga_xIn_{1-x}As$ ternary alloy matched to GaAs is presented. The growth process is described by few heterogeneous chemical equilibria involving gas reactants and the solid component of the alloy. The indium and gallium alloy compositions are then obtained as a function of the substrate temperature, of the reactant fluxes and V/III flux ratio as well as of the strain energy induced by the lattice mismatch. The theoretical results are then compared with experimental composition data obtained by double crystal X-ray diffractions (DCXRD) and by reflection high energy electron diffraction (RHEED) measurements.

INTRODUCTION

In recent years, there has been a growing interest in strained layer superlattices (SLS) and strained multi-quantum well (SMQW) [1–4]. These are high quality multilayered structures grown from lattice mismatched materials. In fact, if the layers are thin enough, no misfit dislocations are generated and a sufficiently high crystalline quality is obtained to allow their use in device applications [5, 6].

In principle, the proper choice of both the substrate and the mismatched layers allows a wider range of tunable properties (relative component concentrations, layer thickness, etc.) which play a fundamental role in the optoelectronics device field.

The molecular beam epitaxy (MBE) technique is widely used to grow films of III–V semiconductors, because of its reliability in controlling the

Correspondence to: M.R. Bruni, ITSE-CNR, c.p. 10000, 16 Monterotondo Stazione, Rome, Italy.

thickness of the growing material as well as its composition. The process of growing epitaxial layers by means of a MBE machine still presents many difficulties due to the great number of parameters which must be controlled during the experiments. As a consequence, a theoretical investigation which is able to give an aprioristic knowledge of the different roles of such parameters could have beneficial feedback on the preparation of materials with increasingly peculiar and modulated properties.

The MBE process can be seen as the resultant of several heterogeneous chemical reactions at the growth front. The kinetics control the evolution of the system towards its equilibrium point with a rate which depends on various dynamical events occurring at the interface (dissociative chemisorption, surface diffusion, bulk incorporation, etc.). If the timescale of each of these processes is small enough with respect to the times connected with the arrival and the evaporation fluxes, a chemical equilibrium can be achieved and this equilibrium is very little affected by the thermal gradients between the substrate and the effusion cells, due to the fast thermal exchange occurring at the growth front [7].

After the pioneering work of Arthur on the vapour phase equilibria in the binary Ga–As systems [8], Heckingbottom [9–11], Seki and co-workers [12–14] and more recently Shen and Chatillon [15] studied the MBE crystal growth of III–V compounds assuming the chemical equilibrium condition and they succeeded in demonstrating that such a very simple model well describes the MBE process.

When an alloy is grown on a substrate with a smaller lattice parameter, as in the case of the $Ga_xIn_{(1-x)}As$ matched to GaAs SLS ($Ga_xIn_{(1-x)}As/GaAs$), the whole structure is elastically strained to take the in-plane lattice parameter a_L very close to the substrate a_0 value. The substrate is then almost unstrained while the alloy sublayer is subject to a compression ($a_L > a_0$) [16].

In a previous paper [17], we reported a preliminary study on ideally matched alloys using a calculation scheme very similar to that of Seki and co-workers [12–14], but using a more analytical procedure. The major advantage of such a procedure, compared with the trial and error procedure of Seki and co-workers, is the higher precision of the numerical results obtained with a very small calculation time.

In the present work we extend this study to the strained $Ga_xIn_{1-x}As$ alloys grown on GaAs substrate. In this case the energetic strain contribution, which can be expressed by the elastic theory of continuous solidi, is taken into account in the calculation of the chemical potentials of the different components of the solid solution.

In the next section we present the calculation procedures used to describe the chemical equilibria occurring in the epitaxial growth of III–V binary and ternary alloy materials. The calculation scheme described for unstrained as well as strained materials is subsequently applied to the

study of the binary alloys GaAs and InAs and to the ternary alloy $Ga_xIn_{1-x}As$.

CALCULATION PROCEDURE

The equilibrium interphase reactions determining the epitaxial growth of III–V binary and ternary compounds may be summarized by a few heterogeneous chemical equilibria, involving the activities of both the gaseous species and the solid components. In this very simple picture, we are then able to fully describe the MBE crystal growth from the knowledge of such activities calculated at the equilibrium point.

In order to achieve this result we have to solve the simultaneous equations of the multiple equilibrium describing the solid formation.

Binary III–V

The chemical reactions involved in the epitaxial growth of the pure binary compounds are described here for the GaAs case

$$2Ga(g) + As_2(g) = 2GaAs(s) \quad (1a)$$

$$4Ga(g) + As_4(g) = 4GaAs(s) \quad (1b)$$

$$As_4(g) = 2As_2(g) \quad (2)$$

Reaction (1b) can be expressed as a linear combination of reactions (1a) and (2), and is thus redundant.

The activity of the pure binary compound is unitary. The equilibrium point is then determined by the values of the three activities of the vapour phase components, which can be considered ideal as a consequence of the high degree of vacuum. The three equations necessary to solve the system are obtained from the equilibrium thermodynamic constants

$$K_1 = 1/P(Ga)^2P(As_2) \quad (3)$$

$$K_2 = P(As_2)^2/P(As_4) \quad (4)$$

and from the global conservation law

$$P^0(Ga) - P(Ga) = P^0(As) - 2P(As_2) - 4P(As_4) \quad (5)$$

where P^0 terms are the input pressures which can be related to the input fluxes by the Knudsen law.

From eqns. (3)–(5), the equilibrium partial pressures are obtained as a function of the input pressures and of the equilibrium constant values

$$P(As_2) = 1/K_1P(Ga)^2 \quad (6)$$

$$P(As_4) = 1/K_1^2K_2P(Ga)^4 \quad (7)$$

where $P(Ga)$ is obtained as a root of the fifth degree equation

$$P(Ga)^5 - [P^0(Ga) - P^0(As)]P(Ga)^4 - (2/K_1)P(Ga)^2 - (4/K_1^2K_2) = 0 \quad (8)$$

which must be solved with the boundary conditions assuring that all the pressure values must be real and greater than zero.

It can be noted that the same solution is obtained by using reaction (1b) instead of reaction (1a). This can be easily proved by solving the equilibrium system with the equilibrium constant

$$K_3 = 1/P(Ga)^4P(As_4) \quad (9)$$

instead of eqn. (3) and taking into account that K_3 is related to K_1 and K_2 by $K_3 = K_1^2K_2$.

Ternary III–III–V

The crystal growth of a III–III–V alloy can be seen as the formation of the two pure binary compounds in the solid solution phase obtained by substituting the two Group III elements in both the two Group III sublattices. This substitution gives rise to an excess Gibbs free energy of the ternary alloy which must be considered in order to calculate the activities of the solid solution components.

Three chemical reactions are necessary in order to fully describe the crystal growth of a III–III–V alloy, here described for $Ga_xIn_{1-x}As$

$$2In(g) + As_2(g) = 2InAs(ss) \quad (10)$$

$$2Ga(g) + As_2(g) = 2GaAs(ss) \quad (11)$$

$$As_4(g) = 2As_2(g) \quad (12)$$

where (ss) indicates the solid solution.

As for the binary case it can be noticed that the reactions of both the Group III elements with the As_4 molecule are redundant. Due to the high degree of vacuum, the partial pressures can be used as activities of all the chemical species in the gas phase. The activities of the solid solution components are expressed by

$$a(InAs)_{ss} = (1 - x)\gamma(InAs)_{ss} \quad (13)$$

$$a(GaAs)_{ss} = x\gamma(GaAs)_{ss} \quad (14)$$

where x is the molar fraction of GaAs in the solid solution phase and γ is the activity coefficient related to the molar partial Gibbs free energy, which for the ith component reads

$$(\partial\Delta G/\partial x_i)_{T,P,xj} = \mu_i = \mu_i^0 + RT \ln x_i + RT \ln \gamma_i \quad (15)$$

where μ_i is the chemical potential and $RT \ln \gamma_i$ the excess free energy ΔG_{exc} of the solid solution.

The excess term ΔG_{exc}, which takes into account of non-ideal behaviour of the solid solution, arises from two major contributions, the mixing energy ΔG_{mx} and for strained structure, the elastic energy ΔG_{st}.

The ΔG_{mx} of the binary alloy can be expressed, as experimentally shown by Stringfellow [18], in accordance with the symmetric regular solution (ideal entropy) [19], as

$$\Delta G_{mx} = \Delta H_{mx} = \Omega x_1 x_2 \tag{16}$$

where x_1 and x_2 are the molar fractions of the two components of the binary solution and Ω is a parameter independent of the composition which takes into account the change of the interaction energy resulting in the Group III sublattice of the alloy with respect to the binary compounds.

The stress resulting from the elastic compression corresponding to the alloy substrate matching produces a change of the free energy which at constant temperature is

$$\Delta G_{st} = 0.5V\boldsymbol{\sigma}\boldsymbol{\varepsilon} - T\Delta S_{st} \tag{17}$$

where V is the volume of the unstrained crystal and $\boldsymbol{\sigma}$ and $\boldsymbol{\varepsilon}$ are the elastic stress and strain tensors respectively.

For an elastic deformation at constant temperature the entropy production coming from the heat redistribution in the lattice is negligible and then the ΔG_{st} is equal to the stored elastic energy.

If the growth of the alloy is along the [001] axis, chosen as the z axis, and the substrate lattice parameter is smaller than the alloy one as in the $Ga_xIn_{(1-x)}As/GaAs$ case, the lattice mismatch induces a compression directed along the growing (x, y) plane and a uniaxial shear along the growth direction. In the hypothesis that the alloy thickness is small enough so that the bending of the uppermost lattice planes can be neglected, all the z components of the stress tensor σ_{xz}, σ_{yz} and σ_{zz} vanish as well as the σ_{xy} component, this latter as a consequence of the quadratic symmetry of the (001) plane.

The whole structure has a strain whose components are

$$\varepsilon_{xy} = \varepsilon_{yz} = \varepsilon_{xz} = 0 \qquad \varepsilon_{xx} = \varepsilon_{yy} = \delta \qquad \varepsilon_{zz} = -2(C_{12}/C_{11})\delta \tag{18}$$

where $\delta = (a_L - a_0)/a_0$ is the strain induced by the lattice mismatch at the interface (alloy–substate), a_L and a_0 are the lattice parameters of respectively the strained and unstrained cells, C_{11} and C_{12} are the second order elastic constants expressed in the usual Voigt notation [20] and ε_{zz} is obtained by

$$\sigma_{zz} = C_{12}\varepsilon_{xx} + C_{12}\varepsilon_{yy} + C_{11}\varepsilon_{zz} = 0 \tag{19}$$

The second order elastic energy density of an anisotropic cubic crystal with isothermal strain directed along the principal axis is in the limits of

generalized Hooke's law [20, 21]

$$W = 0.5C_{11}(\varepsilon_{xx}^2 + \varepsilon_{yy}^2 + \varepsilon_{zz}^2) + C_{12}(\varepsilon_{xx}\varepsilon_{zz} + \varepsilon_{yy}\varepsilon_{zz} + \varepsilon_{xx}\varepsilon_{yy}) \quad (20)$$

and after substituting in eqn. (18), eqn. (20) reads

$$W = \delta^2(C_{11} - C_{12})(C_{11} + 2C_{12})/C_{11} \quad (21)$$

The molar strain free energy is then $\Delta G_{st} = V^0 W$, where $V^0 = Na^3/z$ is the molar volume, N is the Avogadro number and z the number of molecules in the crystalline cell ($z = 4$ for the zincblende structure).

The excess contribution to the chemical potential expressed as usual as the molar partial function is

$$(\mu_i)_{exc} = RT \ln \gamma_i = \Delta G_{exc} + (1 - x_i)(\partial \Delta G_{exc}/\partial x_i)_{T,P} \quad (22)$$

The dependence of ΔG_{st} on the alloy composition results by expressing the lattice parameters and the elastic constants of the alloy as compositional averages of the values of the two binary compounds

$$a = a_1 x_1 + a_2 x_2 \quad (23)$$

$$C_{ij} = (C_{ij})_1 x_1 + (C_{ij})_2 x_2 \quad (24)$$

The lattice parameter values at the temperature T are obtained by performing linear thermal expansions

$$a(T) = a(T^0)[1 + \alpha(T - T^0)] \quad (25)$$

for the two pure binary as well as for the alloy. The thermal expansion coefficient α of the alloy is also obtained by a compositional average $\alpha = \alpha_1 x_1 + \alpha_2 x_2$ as is found experimentally for these materials [22, 23].

The equilibrium point, once γ has been determined, is fully determined by only five variables (x, $P(\mathrm{Ga})$, $P(\mathrm{In})$, $P(\mathrm{As_2})$ and $P(\mathrm{As_4})$), obtained as solutions of the following five independent and simultaneous equations

$$K_1 = [(1 - x)^2/P(\mathrm{In})^2 P(\mathrm{As_2})]\gamma(\mathrm{InAs})^2 \quad (26)$$

$$K_2 = [x^2/P(\mathrm{Ga})^2 P(\mathrm{As_2})]\gamma(\mathrm{GaAs})^2 \quad (27)$$

$$K_3 = P(\mathrm{As_2})^2/P(\mathrm{As_4}) \quad (28)$$

$$P^0(\mathrm{In}) - P(\mathrm{In}) + P^0(\mathrm{Ga}) - P(\mathrm{Ga}) = P^0(\mathrm{As}) - 2P(\mathrm{As_2}) - 4P(\mathrm{As_4}) \quad (29)$$

$$x/(1 - x) = [P^0(\mathrm{Ga}) - P(\mathrm{Ga})]/[P^0(\mathrm{In}) - P(\mathrm{In})] \quad (30)$$

Equations (26)–(28) represent the equilibrium constants relative to the reactions (10–12) respectively, eqn. (29) is the global chemical balance and eqn. (30) is easily deduced from simple stoichiometric considerations.

Two cases can generally appear in order to solve the simultaneous equations (26)–(30).

(i) $\gamma = 1$ case

In the case that the solid solution can be regarded as ideal, both the activity coefficients of the solid components are unitary. The solution of the algebraic system is then obtained as

$$P(\mathrm{Ga}) = \{P^0(\mathrm{Ga}) - [P^0(\mathrm{In}) + P^0(\mathrm{Ga})]x\}k/(k-1)(1-x) \quad (31)$$

$$P(\mathrm{In}) = \{P^0(\mathrm{Ga}) - [P^0(\mathrm{In}) - P^0(\mathrm{Ga})]x\}/(k-1)x \quad (32)$$

$$P(\mathrm{As_2}) = [(k-1)x(1-x)]^2/K_1\{P^0(\mathrm{Ga}) - [P^0(\mathrm{In}) + P^0(\mathrm{Ga})]x\}^2 \quad (33)$$

$$P(\mathrm{As_4}) = (1/K_1^2K_3)[(k-1)x(1-x)]^4/\{P^0(\mathrm{Ga}) - [P^0(\mathrm{Ga}) + P^0(\mathrm{In})]x\}^4 \quad (34)$$

with $k = \sqrt{K_1/K_2}$, P^0 input pressures and with the GaAs solid composition x resulting as a root of the tenth degree equation

$$\sum C_n x_n^{(n-1)} = 0 \qquad (n = 1, 11) \quad (35)$$

The C coefficients only depend on the equilibrium constants K_1, K_2 and K_3 on the input pressures $P^0(\mathrm{In})$, $P^0(\mathrm{Ga})$ and $P^0(\mathrm{As})$ and their complete expressions are reported in the Appendix.

(ii) $\gamma \neq 1$ case

In order to achieve a solution for the transcendental system, the following iterating procedure of subsequent solutions can be adopted. The

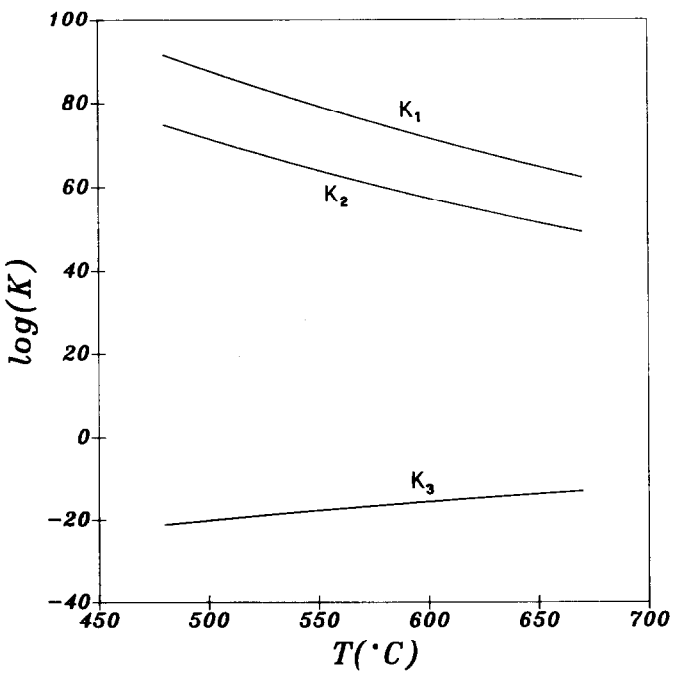

Fig. 1. Values of lg(K) as a function of temperature.

TABLE 1

Lattice constant, second order elastic constants and thermal expansion coefficient for GaAs and InAs

	GaAs	InAs
a (Å) [a]	5.6533	6.0584
C_{11} (10^{11} dyn cm^2) [a]	11.88	8.329
C_{12} (10^{11} dyn cm^{-2}) [a]	5.38	4.526
α (10^{-6} °C^{-1}) [a]	6.63	5.16

[a] See ref. 23 and references cited therein.

activity coefficients γ are firstly set equal to unity and the system is solved as described in the $\gamma = 1$ case. The resulting x, say x^0, will be the zeroth approximant. Such a value is then used in eqn. (22) to compute the activity coefficients γ(GaAs)ss and γ(InAs)ss. At this point $K_1' = K_1/\gamma(\text{InAs})^2$ and $K_2' = K_2/\gamma(\text{GaAs})^2$ are used as equilibrium constant values, to calculate a new solution x'. This procedure is repeated until convergence is reached (the new x differs from that obtained previously by less than a small prefixed value).

Only a few iterations (less than ten) are necessary for all the systems studied here, in order to achieve a convergence of 10^{-4} on the resulting x.

All the thermochemical data used in the calculations of the equilibrium constants have been taken from Show et al. [24], and the Ω values from Panish and Ilegems [25]. The dependence of K_1, K_2 and K_3 on temperature are shown in Fig. 1. The physical constants required in the calculation of the strain component of the activity coefficient are specified for the two binary systems GaAs and InAs in Table 1.

RESULTS AND DISCUSSION

Figure 2 shows the normalized growth rate computed for the two binary compounds GaAs and InAs as a function of the temperature and at various input pressures P_V^0/P_{III}^0 (V/III) ratios.

The normalized growth rates, expressed versus the Group III elements as $r = (P_{III}^0 - P_{III})/P_{III}^0$, have been calculated from the equilibrium pressure values obtained as previously described in the section headed Calculation procedure.

As it can be noted in Fig. 2, the different curves corresponding to different values of V/III ratios (0.1–100) show a similar trend independently of the V/III ratio values. At first, the curves are linear and almost parallel to the temperature axis. At higher temperatures, a rapid decrease towards negative values ("etching zone") can be observed. The first linear trend of the growth rates at lower temperatures indicates that reactions (1a) are complete due to their high exothermicity. The growth ends as a

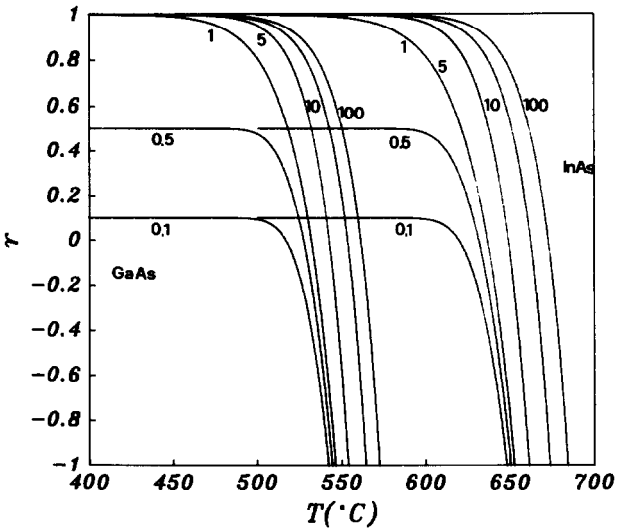

Fig. 2. Theoretical normalized growth rates of binary GaAs and InAs as a function of the temperature. $P^0_{III} = 3.9 \times 10^{-7}$ Torr and V/III ratio ranging from 0.1 to 100.

consequence of the disappearance of the less abundant reactant in the gas phase (either Group V molecules for V/III values less than unity or Group III atoms for larger values). The calculated equilibrium pressure of such reactants in this zone falls below the value of $P = 10^{-20}$ Torr as the temperature decreases. In this case it is quite hard to talk about a chemical equilibrium even if a mathematical solution of the system (3)–(5) is still correctly obtained.

As the temperature increases the equilibrium moves towards the gas phase (endothermic reaction) and becomes much more sensitive to the partial pressures of the reactants in the gas phase.

As it can be seen in Fig. 2, the temperatures at which the growth rate starts decreasing increases a little with a Group III excess and this is a consequence of the quadratic dependence of the equilibrium constant (see eqn. (1a)) on the Group III pressure. Otherwise, the temperatures at which the growth rates become zero (sublimation temperatures) increase with the V/III ratio. This is mainly due to the higher total pressure which results for the larger V/III ratio values (P^0_{III} is kept constant and equal to 3.9×10^{-7} Torr for all the curves in Fig. 2).

From the chemical equilibrium point of view it follows that the growth of a binary III–V compound is improved by a higher pressure of both the Group III and the Group V reactants. This result partially disagrees with most of the experimental knowledge from which it is evident that growth of binary III–V materials cannot be obtained if a Group III overpressure is present [26, 27].

To explain this disagreement, additional reactions such as the Group III

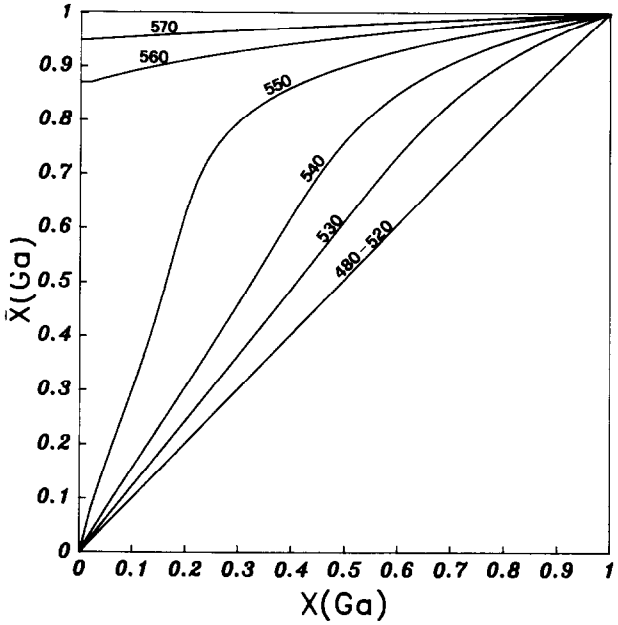

Fig. 3. Theoretical solid compositions of $Ga_xIn_{(1-x)}As$ versus the Ga input gas phase composition. $P^0_{III} = 3.9 \times 10^{-7}$ Torr and V/III ratio = 27. The curves are calculated using temperatures in the range 480–570°C.

atoms clustering on the growing surface [28], together with those studied here, should be taken into account.

In Fig. 3 the compositional curves, expressed as the molar fraction of GaAs in the alloy, indicated as X(Ga), versus the input gas phase Group III composition X(Ga), are reported. The equilibrium values of X(Ga) are calculated for the alloy $Ga_xIn_{(1-x)}As$ at temperatures ranging from 480–570°C. It must be pointed out that the results of Fig. 3 are relative to the formation of an ideally matched alloy and, then, the strain energy does not contribute to the calculation of the activity coefficients.

As can be seen by comparing the curves relative to the different temperatures, the composition of the alloy is strongly affected by the temperature and consequently by the different endothermicities of the two binary compound formed (see reactions (10) and (11)). At the lower temperatures (T = 480–520°C), both reactions can be considered almost complete versus the solid formation; then the relative amount of GaAs and InAs in the alloy depends only on the initial composition of the reactants in the gas phase. The curves of Fig. 3 are, in this case, very close to a straight line with a slope equal to unity.

As the temperature increases ($T > 570$°C) the less exothermic reaction (11) becomes predominant with respect to reaction (10). As a consequence the GaAs content of the alloy increases until it can be considered equal to unity for any input composition.

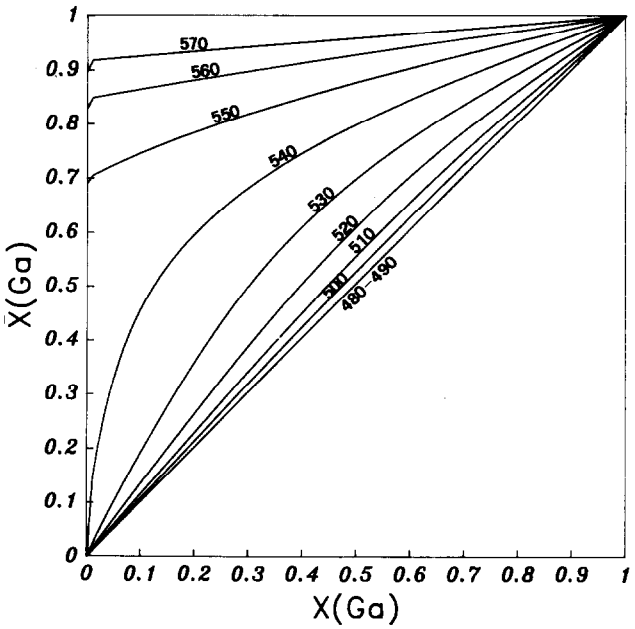

Fig. 4. Theoretical solid compositions of $Ga_xIn_{(1-x)}As/GaAs$ versus the Ga input gas phase composition. $P^0_{III} = 3.9 \times 10^{-7}$ Torr and V/III ratio = 27. The curves are calculated using temperatures in the range 480–570°C.

For each intermediate temperature, alloys in the whole composition range are obtained.

The influence of the lattice mismatch on the composition of the growing $Ga_xIn_{(1-x)}As/GaAs$ alloy is shown in Fig. 4 where the compositional curves are as reported in Fig. 3 but the strain contribution has been taken into account in the calculation of the activity coefficients.

By comparing the curves of Figs. 3 and 4, it is clearly seen that in the latter case the alloys are less rich in InAs. Higher loads of the components with larger lattice parameters are avoided because of the ΔG_{exc} increase as a consequence of the larger strain.

In Figs. 5 and 6 the compositional curves calculated for the alloys $Ga_xIn_{(1-x)}As$ and $Ga_xIn_{(1-x)}As/GaAs$ at $T = 530$°C and with P^0_{III} ranging between 1.0×10^{-7} Torr and 5.0×10^{-7} Torr are shown. The discussion of the results relative to Figs. 5 and 6 is very similar to those of Figs. 3 and 4 respectively. However in this case, as can be seen, an increase of pressure produces the same result as a decrease of temperature. Higher pressures always move the equilibrium towards the solid phase until the alloy formation reaction can be considered almost complete. In this situation the different exothermicities of the reactions (10) and (11) can be neglected and, then, higher incorporations of InAs are possible.

Figure 7 shows the calculated compositional curves of the $Ga_xIn_{(1-x)}As$ and $Ga_xIn_{(1-x)}As/GaAs$ in comparison with some experimental results.

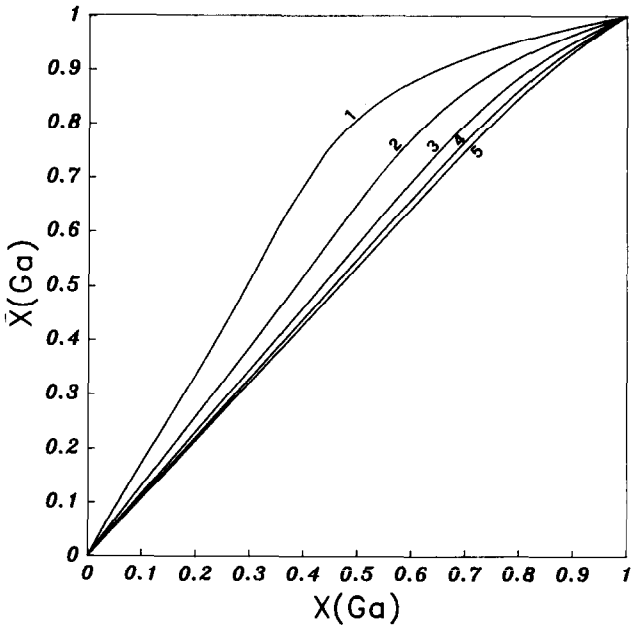

Fig. 5. Theoretical solid compositions of $Ga_xIn_{(1-x)}As$ as a function of the Group III total pressure. $T = 530°C$ and V/III = 27. The numbers on the curves refer to the P^0_{III} value expressed in 10^{-7} Torr.

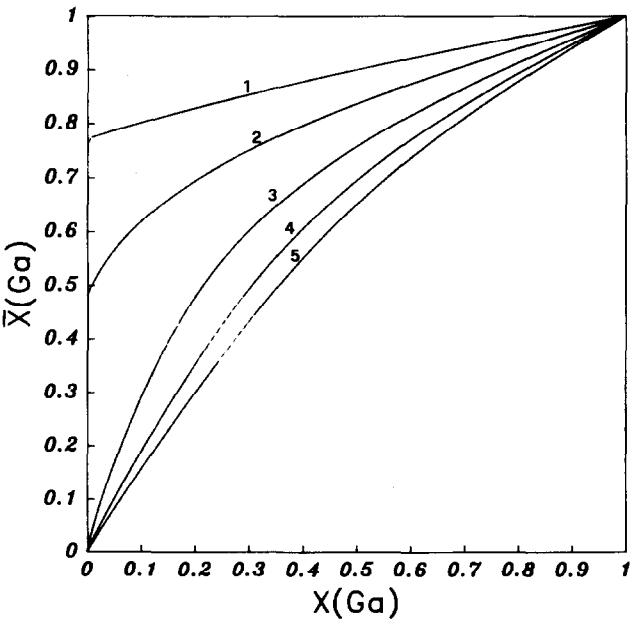

Fig. 6. Theoretical solid compositions of $Ga_xIn_{(1-x)}As/GaAs$ as a function of the Group III total pressure. $T = 530°C$ and V/III = 27. The numbers on the curves refer to the P^0_{III} value expressed in 10^{-7} Torr.

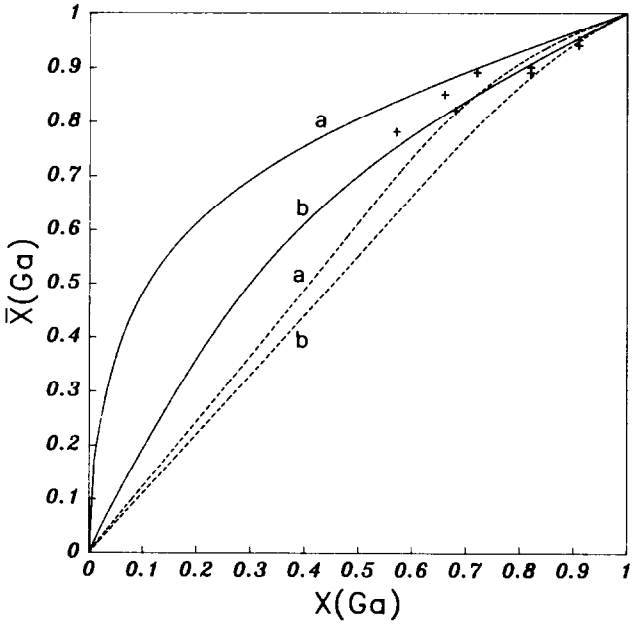

Fig. 7. Experimental (points marked with +) and calculated compositions of $Ga_xIn_{(1-x)}As/GaAs$ (solid lines) and $Ga_xIn_{(1-x)}As$ (broken lines) versus the Ga input gas phase compositions. The experimental data are taken from refs. 26 and 27. $P^0_{III} = 3.9 \times 10^{-7}$ Torr, V/III = 27.

All the materials, to which the experimental points of Fig. 7 refer, were grown on GaAs substrate by a MBE GENII Varian machine [29, 30] and their composition has been evaluated by measurements of the oscillations of the reflection high energy electron diffraction (RHEED) intensities. The results of the different measurements are reported in Table 2 together with some other experimental data.

The two series of curves shown in Fig. 7 refer to the two different cases of strained (solid lines) and unstrained (dashed lines) materials. The equilibrium compositions of the alloys have been calculated at the same temperature $T = 530$°C used for the experimental growth as reported in refs. 29 and 30 with a V/III ratio equal to 27, very close to the averaged values of the experimental ratios employed and using $P^0_{III} = 2.37 \times 10^{-7}$ Torr (curve a) and $P^0_{III} = 3.9 \times 10^{-7}$ Torr (curve b) for the two curves of each series. These pressures correspond to the minimum and maximum values in the range in which the experimental pressures are spread as reported in Table 2.

As it can be seen in Fig. 7 and taking into account the experimental uncertainty of the measurement techniques, there is a good agreement between the experimental compositions and those calculated for the $Ga_xIn_{(1-x)}As/GaAs$. The comparison between the alloy compositions obtained by double crystal X-ray diffraction (DCXRD) and RHEED

TABLE 2

Experimental data (see text) [a]

Sample [b]	P^0_V/P^0_{III}	P^0_{III}	$P^0_{(Ga)}/P^0_{III}$	$X_{(Ga)}$	
				DCXRD	RHEED
S12	26	3.67	0.72	0.88	0.80
S11	26	3.61	0.72	0.88	0.80
S13	27	3.58	0.72	0.88	0.80
S15	30	2.65	0.82	0.90	0.89
S21	25	2.60	0.82	0.90	0.89
S22	29	2.60	0.82	0.90	0.89
S27	31	2.50	0.82	0.90	0.89
S14	23	3.10	0.68	0.81	0.77
S16	30	2.37	0.91	0.94	0.93
S23	27	2.60	0.57	0.77	0.73
S29	25	3.90	0.66	0.85	0.81
S31	35	2.50	0.82	0.89	0.87
S34	32	2.60	0.82	0.89	0.87
S35	36	2.40	0.91	0.95	0.94

[a] Pressures are expressed in 10^{-7} Torr; $T = 530$°C. [b] See Refs. 29 and 30.

measurements, as reported in Table 2, shows that from the latter measurements a higher load of InAs in the alloys always results. This can be attributed to the kinetic formalism of the growth rates obtained by RHEED measurements and their use in the calculations of the alloy compositions. In this case the relevant influences of the different activities of the alloy components and their dependence on the strain energy are not taken into account properly.

It emerges quite clearly either from the literature or the present work that the chemical equilibrium formalism seems to be able to describe in a satisfactory way the epitaxial growth of the III–V materials and that it agrees well with available experimental results.

It must be stressed, at this point, that the agreement between the experimental and the theoretical results goes beyond the composition of the alloys. In fact the calculations here reported are able to predict in a quite exact manner the experimentally used values of relevant growth parameters such as the substrate temperature and the Group III pressure [29–32] and this occurs in spite of the strong influence of such parameters on the growth process.

It might even be possible to improve the agreement between theoretical and the experimental results by using in the calculations of the equilibrium constants more accurate values of the thermochemical parameters.

It can be pointed out that a virtue of the present calculation is that is has been carried out independently of any experimental results. In view of

this, the predictive power of the calculations about both the growth parameters such as the temperatures and pressures used in the experiments and the resulting compositions of the grown alloys must be considered significant and it gives a measure of support to the chemical equilibrium formalism.

CONCLUSIONS

A thermodynamic study based on chemical equilibrium calculations has been presented for the MBE growth of GaAs and InAs binary compounds and their alloys $Ga_xIn_{(1-x)}As$, both unstrained and strained by the mismatch to the substrate.

The theoretical results have been compared with some experimental composition data obtained by DCXRD measurements on samples of $Ga_xIn_{(1-x)}As$ matched to GaAs.

From this comparison it is shown that the calculated equilibrium compositions agree well with the experimental data whenever the strain energy is taken into account in the calculation of the Gibbs free energy of the alloy. This agreement indicates the validity of the chemical equilibrium treatment of the MBE process and how much such a simple formalism provides a useful and powerful guide for MBE growth.

ACKNOWLEDGEMENTS

This work was partially supported by the Progetto Finalizzato Materiali Speciali del CNR. The authors thank F. Martelli and M. Zugarini for their help in the growth experiments, C. Ferrari for performing the DCXRD measurements and A.A. Bonapasta for helpful discussions.

REFERENCES

1 L. Esaki and R. Tsu, IBM J. Res. Dev., 14 (1970) 61.
2 J.W. Matthews and A.E. Backeslee, J. Cryst. Growth, 27 (1974) 118.
3 G.C. Osbourne, IEEE J. Quantum Electron., QE-22 (1986) 1677.
4 B. Jogai and P.W. Yu, Phys. Rev. B, 41 (1990) 12650.
5 I.J. Fritz, P.L. Gourley and L.R. Dawson, Appl. Phys. Lett., 51 (1987) 1004.
6 T.G. Andersson, Z.G. Chen, V.D. Kulakoskii, A. Uddin and J. Vallin, Appl. Phys. Lett., 51 (1987) 752.
7 J.R. Arthur and T.R. Brown, J. Vac. Sci. Technol., 20 (1975) 200.
8 J.R. Arthur, J. Phys. Chem. Solids, 28 (1967) 2257.
9 R. Heckingbottom, J. Vac. Sci. Technol. B, 3 (1985) 572.
10 R. Heckingbottom, J. Electrochem. Soc., 127 (1980) 444.
11 R. Heckingbottom, G.J. Davies and K.A. Prior, Surf. Sci., 132 (1983) 375.
12 H. Seki and A. Koukitu, J. Cryst. Growth, 78 (1986) 342.
13 H. Seki and A. Koukitu, J. Cryst. Growth, 74 (1986) 172.
14 A. Kouktu, H. Nakai, T. Suzuki and H. Seki, J. Cryst. Growth, 84 (1987) 425.
15 J. Shen and C. Chatillon, J. Cryst. Growth, 106 (1990) 553.

16 J.Y. Martin, in ed: G. Allan, G. Bastard, N. Boccara, M. Lannoo and M. Voos (Eds.), Heterojunctions and Semiconductors Superlattice, Springer-Verlag, Berlin, 1986, p. 161.
17 M.R. Bruni, A. Lapiccirella, G. Scavia, M.G. Simeone, S. Viticoli and N. Tomassini, in A. D'Andrea, A. Lapiccirella, G. Marletta and S. Viticoli (Eds.), Materials for Photonic Devices, World Scientific, Singapore, 1991, p. 63.
18 G.B. Stringfellow, J. Crystal Growth, 27 (1974) 21.
19 J.H. Hildebrand and E.J. Salstrom, J. Am. Chem. Soc., 54 (1932) 4257.
20 C. Teodosiu, Elastic Models of Crystal Defects, Springer-Verlag, Berlin, 1982.
21 C. Kittel, in Introduction to Solid State Physics, Wiley, New York, 1967, p. 110.
22 R. Bisaro, P. Merenda and T. Pearsall, Appl. Phys. Lett., 34 (1979) 10.
23 S. Adachi, J. Appl. Phys., 53 (1982) 8775.
24 D.H. Show, J. Phys. Chem. Solids, 36 (19751) 111.
25 M.B. Panish and M. Ilegems, in H. Reiss and J.O. McCaldin (Eds.), Progress in Solid State Chemistry, Pergamon, New York, 1972, pp. 39–83.
26 B.R. Honcock and H. Kromer, J. Appl. Phys., 55 (1984) 4239.
27 T. Nakagara, S. Gonda and S. Emura, J. Cryst. Growth, 87 (1988) 276.
28 S.V. Ivanov, P.S. Kop'ev and N.N. Ledenstov, J. Cryst. Growth, 104 (1990) 345.
29 M.R. Bruni, F. Martelli, M.G. Proietti, M.G. Simeone and M. Zugarini, J. Appl. Phys., 71 (1992) 539.
30 M.R. Bruni, C. Ferrari, F. Martelli, M.G. Proietti and m.G. Simeone, J. Cryst. Growth, in press.
31 E.C. Colin, D. Wood, V. Morgan and L. Rathbun, J. Appl. Phys., 53 (1982) 4524.
32 M. Quillec, L. Goldstein, G. LeRoux, J. Burgeat and J. Primot, J. Appl. Phys., 55 (1984) 4524.

APPENDIX

The C coefficients of eqn. (35) are expressed as

$$C_n = A_n - B_n(k-1)^3$$

with $k = \sqrt{K_1/K_2}$ and

$$A_1 = -P^0(\mathrm{Ga})^5$$

$$A_2 = P^0(\mathrm{Ga})^4\{k[P^0(\mathrm{In}) - P^0(\mathrm{As})]\} + P^0(\mathrm{In}) + 2P^0(\mathrm{Ga}) + P^0(\mathrm{As})$$

$$A_3 = P^0(\mathrm{Ga})^3\{P^0(\mathrm{Ga})P^0(\mathrm{As}) - 4[kP^0(\mathrm{In}) - kP^0(\mathrm{As}) + P^0(\mathrm{Ga}) + P^0(\mathrm{As})] \times 6[P^0(\mathrm{In}) + P^0(\mathrm{Ga})]^2\}$$

$$A_4 = P^0(\mathrm{Ga})^2\{-4P^0(\mathrm{Ga})P^0(\mathrm{As})[P^0(\mathrm{In}) + P^0(\mathrm{Ga})] + 6[kP^0(\mathrm{In}) - kP^0(\mathrm{As}) + P^0(\mathrm{Ga}) + P^0(\mathrm{As})][P^0(\mathrm{In}) + P^0(\mathrm{Ga})]^2 + 4[P^0(\mathrm{In}) + P^0(\mathrm{Ga})]^3\}$$

$$A_5 = P^0(\mathrm{Ga})\{6P^0(\mathrm{Ga})P^0(\mathrm{As})[P^0(\mathrm{In}) + P^0(\mathrm{Ga})]^2 - 4[kP^0(\mathrm{In}) - kP^0(\mathrm{As}) + P^0(\mathrm{Ga}) + P^0(\mathrm{As})] \times [P^0(\mathrm{In}) + P^0(\mathrm{Ga})]^3 - [P^0(\mathrm{In}) + P^0(\mathrm{Ga})]^3\}$$

$$A_6 = -4P^0(\mathrm{Ga})P^0(\mathrm{As})(k-1)[P^0(\mathrm{In}) + P^0(\mathrm{Ga})]^3 \cdot$$
$$+ [kP^0(\mathrm{In}) - kP^0(\mathrm{As}) + P^0(\mathrm{Ga}) + P^0(\mathrm{As})][P^0(\mathrm{In}) + P^0(\mathrm{Ga})]^4$$

$$A_7 = P^0(\mathrm{As})(k-1)[P^0(\mathrm{Ga}) + P^0(\mathrm{In})]^4$$

$$A_8 = A_9 = A_{10} = A_{11} = 0$$

and

$$B_1 = B_2 = B_3 = 0$$

$$B_4 = 2P^0(\mathrm{Ga})^2/K_1$$

$$B_5 = [4P^0(\mathrm{Ga})P^0(\mathrm{In}) + 10P^0(\mathrm{Ga})^2]/K_1$$

$$B_6 = \{-[2P^0(\mathrm{In})^2 + 16P^0(\mathrm{In})P^0(\mathrm{Ga}) + 14P^0(\mathrm{Ga})^2]/K_1\}$$
$$- (4/K_1^2K_3)(k-1)^2$$

$$B_7 = \{[6P^0(\mathrm{In})^2 + 10P^0(\mathrm{Ga})P^0(\mathrm{In}) + 18P^0(\mathrm{Ga})^2]/K_1\}$$
$$+ (20/K_1^2K_3)(k-1)^2$$

$$B_8 = \{-[6P^0(\mathrm{In})^2 + 16P^0(\mathrm{Ga})P^0(\mathrm{In}) + 10P^0(\mathrm{Ga})^2]/K_1\}$$
$$- (40/K_1^2K_3)(k-1)^2$$

$$B_9 = 2[P^0(\mathrm{Ga}) + P^0(\mathrm{In})]^2/K_1 + (40/K_1^2K_3)^2(k-1)^2$$

$$B_{10} = (-20/K_1^2K_3)^2(k-1)^2$$

$$B_{11} = (4/K_1^2K_3)(k-1)^2$$